Electrical conductivity measurements as proxies for diffusion-limited microbial activity in soils under controlled laboratory conditions.

Orsolya Fülöp[1,2], Naoise Nunan[2,3], Mamadou Gueye[2], Damien Jougnot[1]

[1] Sorbonne Université, CNRS, EPHE, UMR 7619 METIS, F-75005 Paris, France
[2] Sorbonne Université, CNRS, IRD, INRAE, UPEC, Institute of Ecology and Environmental Sciences – Paris, F-75005 Paris, France
[3] Department of Soil and Environment, Swedish University of Agricultural Sciences, Uppsala, Sweden

Correspondence to: Naoise Nunan (naoise.nunan@cnrs.fr)

Short summary:

Soil microorganisms exist in a highly structured, variably connected environment, where they play a critical role in organic matter dynamics. To investigate the relationship between soil respiration and the connectivity of the soil pore water phase, we studied the use of electrical conductivity as a proxy for soil respiration. Our results show that there were non-linear relationships between the two variables, thereby opening up a new approach to better understand soil respiration.

Abstract:

Soils play a dynamic role in the carbon cycle, functioning as both a source and a sink for atmospheric carbon. Despite their importance, uncertainties in soil-atmosphere interactions persist due to the complex processes governing soil carbon dynamics. Microbial access to substrate is a key mechanism regulating organic C decomposition. Evidence suggests this access is diffusion-limited, as reflected in the strong dependence of soil respiration on water availability. In recent years, non-destructive geophysical tools, including electrical conductivity measurements, have been used to determine the water content of soils and the connectedness of the water phase in the soil pore network. As both respiration and electrical conductivity may depend on water availability and connectivity, our study aimed to determine whether electrical conductivity measurements could serve as a proxy for soil respiration when microbial activity is potentially diffusion-limited. This was done by measuring electrical conductivity and respiration rates at different matric potentials, using sieved and undisturbed top- and subsoil samples taken from conventional tillage and conservation agriculture management plots of a Luvisol. Our results revealed an initial increase followed by a subsequent decrease in soil respiration with increasing matric suction (i.e., decreasing water saturation). Electrical conductivity decreased as the soil desaturated. The two variables exhibited a significant nonlinear relationship, indicating a shared sensitivity to changes in aqueous phase connectivity. Finally, a quantitative approach for estimating the tortuosity of the water phase in the samples, based on the electrical conductivity measurements, was used to show a clear relationship between water phase tortuosity and respiration measurements. These results thus suggest that both measured variables depend on the connectedness of the aqueous phase and highlight the potential of electrical conductivity measurements as a mechanistically informed proxy for diffusion-constrained soil respiration.

Keywords: Soil respiration, Microbial activity, Carbon cycle, Diffusion limitation, Water availability, Electrical conductivity, Pore connectivity, Soil moisture, Tortuosity

1. Introduction

Natural soils contain the most diverse terrestrial microbial communities as well as terrestrial organic carbon reserves with quantities surpassing those found in both the atmosphere and vegetation combined (Crowther et al., 2019; Dubey et al., 2020). Through microbial processing of organic inputs, soils function either as a carbon sink or a source, depending on the balance between carbon inputs and losses (Hargreaves et al., 2015; Six et al., 2006). Carbon (C) inputs are processed by microbial communities and are either released to the atmosphere as CO_2 or converted into microbial biomass and ultimately soil organic matter (Al-Maliki & Ebreesum, 2020; Fan et al., 2015; Sandor et al., 2020). Several factors modulate soil C dynamics, including the intrinsic resistance of organic molecules to decomposition, the spatial inaccessibility of organic matter (OM) to microbial decomposers, and organo-mineral associations (Lützow et al., 2006). Because decomposition occurs when organic molecules encounter microbial decomposers or their extracellular enzymes (Dignac et al., 2017), the spatial separation of OM and decomposers is considered a major constraint, as microorganisms and OM are heterogeneously distributed and occupy only a small fraction of the soil pore system (Dignac et al., 2017; Lützow et al., 2006). Thus, decomposition requires the movement of substrates, microorganisms, or both.

A relatively small proportion of soil microbial communities possess flagellar motility, primarily in zones with high OM content (Ramoneda et al., 2024), such as the rhizosphere. Microbial decomposition of OM therefore largely relies on the diffusion of organic molecules toward decomposers (Nunan et al., 2020). Diffusion limitation is supported by observations that OM decomposition often varies linearly with the square root of time, a characteristic of diffusion-controlled processes (Stanford & Smith, 1972). Because substrate diffusion occurs only in the presence of water, partially saturated soils require continuity of the aqueous phase across connected pores (Lang et al., 2007). Respiration declines sharply at low water contents (Davidson et al., 1998), highlighting the central role of water availability in regulating microbial activity (Kpemoua et al., 2023; Nasiri et al., 2023). However, the mechanistic hierarchy underlying this relationship remains unclear. In partially saturated soils, diffusion limitation arises not only from reduced water content but also from loss of continuity in the water-filled pore network, which increases tortuosity and constrains substrate diffusion through the aqueous phase (Ghanbarian et al., 2013; Ebrahimi & Or, 2015; Ghezzehei et al., 2019).

Geophysical methods are increasingly applied as fast, non-destructive approaches to monitor soil moisture dynamics (Garre et al., 2021; Hermans et al., 2023; Loiseau et al., 2023) and to infer water-phase connectivity in porous media (Li et al., 2015; Jougnot et al., 2018; Wilson et al., 2024). Electrical conductivity (EC) measurements are particularly sensitive to connectivity within the aqueous phase, through which charge carriers move, enabling characterization of pore spaces supporting solute diffusion (Jougnot et al., 2009; Revil & Jougnot, 2008). When measured across a range of soil matric potentials (i.e., water contents), EC responds to changes in aqueous phase continuity and tortuosity that control diffusive transport. Accordingly, EC

is widely used to monitor spatial and temporal variations in the connectivity of the water-filled pore space(Garre et al., 2021; Hermans et al., 2023).

With both respiration and electrical conductivity potentially relying on the diffusion of either substrates or charge carriers across soil systems, this raises the question of whether electrical conductivity measurements could act as a proxy for soil respiration in the absence of water flow. Different soil matric potentials correspond to different water contents, which alter pore connectivity and tortuosity and therefore influence diffusion-controlled transport processes (Revil and Jougnot, 2008; Ghanbarian et al., 2013; Jougnot et al., 2018).

To address this question and improve our understanding of the relationship between microbial respiration and diffusion, this study aimed to investigate the relationship between soil respiration and electrical conductivity across a range of soil matric potentials. This relationship was examined to evaluate a novel methodology for the rapid characterization of soil biological processes. Measurements were conducted on both sieved and undisturbed topsoil and subsoil samples from two treatments of a long-term field trial.

Our primary hypothesis was that under diffusion-limited conditions, microbial respiration rates are positively correlated with electrical conductivity due to their shared dependence on diffusive transport. We further hypothesized that higher initial carbon availability would weaken this relationship, as a broader distribution of organic substrates reduces diffusion constraints. In this context, we expected differences between topsoil and subsoil samples to emerge. Finally, we hypothesized that sieving homogenizes the pore network, resulting in more consistent relationships between electrical conductivity and respiration than those observed in undisturbed soil samples.

2. Material and Methods

2.1. Study site and sample collection

The soil used in the study was collected from the “La Cage” field experiment on the French National Institute for Agricultural Research (INRAE) campus in Versailles, Ile-de-France (48°45’N; 2°08’E). The climate of the greater Parisian basin is characterized as temperate, with an average precipitation of 630 mm and an annual average temperature of 10.4 °C (Bellone et al., 2023). The experimental site was established in 1998 to conduct long-term field studies on the effects of different cultivation methods on a well-drained Luvisol soil (Autret et al., 2020). Soil from two treatments, conventional tillage and conservation agriculture, were tested. The conventional tillage site underwent annual ploughing to a depth of 30 cm and systematic pesticide application. In contrast, the conservation agriculture treatment was not tilled and was maintained with persistent cover crops. Pesticides were applied only when plant damage was detected in the conservation agriculture treatment.

Both fields were under plant cover at the time of sampling in early November 2023. This cover corresponded to mustard in the case of the conventional tillage field, and common vetch and black oats for the conservation agriculture field. The main

crops consisted of a wheat-pea-rapeseed crop rotation for the conventional tillage site and pea-wheat-corn-oat rotation for the conservation tillage site. A more detailed description of the plant cover and management practices is provided in Autret et al. (2016). The choice to use the conventional tillage and conservation agriculture treatments was based on the expectation that these would have different soil structures and C contents, both key factors influencing carbon dynamics. The selection of these two systems is supported by findings from the La Cage study, which show that conservation agriculture generally sustains higher microbial biomass, total C, and significantly greater stabilized soil organic carbon content compared to conventional tillage (Henneron et al., 2015; Juarez et al., 2013). Further studies have identified the presence of more stable water-soluble aggregates and associated improved porosity in the conservation agriculture fields compared to conventional tillage treatments (Chabert & Sarthou, 2020; Cosentino et al., 2006). This improved aggregate stability is expected to influence the maintenance of pore connectedness across a range of matric potentials (Mondal & Chakraborty, 2022).

To obtain a wide range of pore size distributions, pore connectivity, carbon contents and microbial biomass, we used sieved (<2 mm) and undisturbed samples from the topsoil (0–15 cm) and subsoil (50 cm). The soil microbial biomass and soil C contents are known to decrease with depth of the soil profile (Salomé et al., 2010) and sieving changes the physical structure and water retention properties of soil (Herbst et al., 2016).

The undisturbed samples were collected by inserting PVC sampling cores (80 mm in length and 58 mm in internal diameter) directly into the soil horizons and carefully extracting them to preserve soil structure. All undisturbed samples were frozen at -20°C until use to minimize organic matter decomposition during storage prior to incubation experiments (Allende-Montalbán et al., 2024). Bulk soil collected to prepare sieved samples was air-dried, sieved to 2 mm, and stored at 10°C until the experiment began.

2.2 Sample preparation for incubation

Undisturbed samples were thawed gradually by transferring them from a deep freezer to an 8 °C refrigerator for 24 hours, followed by five days at 20 °C in the laboratory prior to incubation. Sieved samples were prepared by packing soil to a target bulk density of 1.73 g cm^{-3}, corresponding to the average bulk density measured in undisturbed samples. Because the undisturbed cores were collected under very wet field conditions, some disturbance during sampling may have affected the measured bulk density. This bulk density value was therefore used only to obtain comparable soil mass and pore volume between treatments and not to reproduce the in situ soil structure.

Samples were saturated by capillary rise by initially placing them in 1 cm of water, with additional water added gradually over 24 hours until full saturation was achieved. The samples were then transferred to airtight microcosms and incubated in the dark to limit algal growth on the microcosm surface caused by light exposure.

2.3. Study approach and incubation set-up

This study examined the effect of soil water status on respiration rates and electrical conductivity during short-term incubations. To impose different soil water contents without physically disturbing the samples, matric potentials of -70, -100, -250, -350, -450 and -630 hPa were applied using a suction system. The corresponding conversion between matric potentials and water content is described in Section 2.4.3.

Samples were placed in airtight microcosms fitted with a ceramic plate allowing adjustment of the pressure head and a septum for headspace sampling (Poll et al., 2010; Fig.1). The ceramic plate positioned at the base of each microcosm was connected to a suction pump, enabling precise pressure-head control of the soil cores. Additionally, an opening in the lid was used to route electrical cables for conductivity measurements. A schematic of the setup is provided in Fig. S1.

Five microcosms at a time were subjected to controlled suction, and drained water was collected in refrigerated bottles at 4 °C for subsequent analysis of soil solution ionic strength. One microcosm was used exclusively for gravimetric measurements to verify changes in moisture content. Each treatment was performed in triplicate.

Incubations were conducted at 20 °C. Samples were maintained at each pressure head for approximately 24 hours after leaching had ceased to allow hydraulic equilibrium to be reached. In total, 24 microcosms were used (four soils × two structural treatments × three replicates). Samples were analysed in randomized order such that replicates from the same soil and treatment combination were not measured simultaneously.

After measurements at -630 hPa were completed, samples were transferred to mason jars fitted with septa for headspace sampling and containing an oversaturated lithium chloride solution. This induced a suction at the sample surface corresponding to a pressure head of -996 hPa (Colas, 2011.; Greenspan, 1977). Sample weights were monitored periodically until no further mass loss was observed, indicating that the target pressure head had been reached.

2.4 Analytical data collection

2.4.1 CO_2 flux measurements

Soil respiration rates were measured by taking four gas samples (20 mL each) from the microcosm headspace at each applied matric potential. CO_2 concentrations were analysed using a micro gas chromatograph (micro-GC, Agilent 3000). The instrument was equipped with a PLOT Q column (Poropak Q) to separate CO_2 from other gases, and helium was used as the carrier gas. Detection was performed with a thermal conductivity detector (TCD). Respiration rates were calculated from the increase in CO_2 concentration over time. Additional details of the microcosm and gas sampling setup are shown in Fig. S1.

For the characterization of the soil respiration flux, the slope of CO_2 accumulation over time was determined by linear regression (R base stats package) and visualized using ggplot2 (v. 4.0.1). Specifically, the respiration flux (FCO_2) was obtained as the slope of the linear regression of CO_2 concentration (C, ppm) against time (t, s):

$$F_{CO_2} = \frac{dC}{dt}. \quad (1)$$

The flux per gram of organic matter (F_{OM}) was then calculated as,

$$F_{OM} = \frac{F_{CO_2}}{m_{OM}}, \quad (2)$$

where m_{OM} is the organic matter mass (g) in each sample.

For the visualization of the soil respiration rate, we used the relative soil respiration (F_{rel}) as the ratio of the flux at the given condition to the flux at -70 hPa,

$$F_{rel} = \frac{F_{OM}}{F_{OM(-70hPa)}}. \quad (3)$$

The −70 hPa condition was used as the reference, corresponding to the highest water content treatment.

2.4.2 Electrical Conductivity Measurements

Sample electrical conductivity was monitored using a PSIP unit (Portable Spectral Induced Polarisation, Ontash and Ermac; ontash.com) in parallel with soil respiration measurements. The PSIP unit was fitted to a custom-made electrode configuration for each sample. A voltage of 5 V was imposed between the current injection electrodes, and the real part of the complex conductivity at 1 Hz was recorded and averaged over five periods. A frequency of 1 Hz was used, as this is the most commonly employed frequency for electrical conductivity measurements in field studies (e.g., Blanchy et al., 2025).

The PVC cores were fitted with brass screws, 1.5 mm in diameter and 16 mm in length, which served as electrodes. The electrode configuration and corresponding geometrical factors were determined using COMSOL Multiphysics 5.0 and are shown in the Supplementary Material (Fig. S2). Each electrode was inserted 6 mm into the soil cores to ensure consistent soil contact and to minimize the effects of minor shrinkage caused by moisture loss at the sample edges.

Injection electrodes were positioned at the top and bottom of the samples, while three pairs of potential electrodes were inserted vertically and one pair horizontally to capture a broader distribution of current lines within the sample. Electrical conductivity was calculated using the geometrical factors listed in Table S1 of the Supplementary Material.

For the electrical conductivity analysis, the estimated soil water saturation (S_w) was used for each sample. Bulk electrical conductivity was fitted using the following pedophysical relationship (Waxman & Smits, 1968),

$$\sigma = \frac{S_w^n}{F}(\sigma_w + \frac{\sigma_s}{S_w}), \quad (4)$$

where S_w is water saturation (-), F the formation factor (-), n the saturation exponent (-), σ_w the pore water conductivity (S/m), and σ_s the surface conductivity (S/m). Model parameters were estimated using nonlinear least squares fitting.

This fitting procedure also allowed the estimation of tortuosity, τ_w (-), as a function of water saturation following Jougnot et al. (2018),

$$\tau_w = \Phi F S_w^{(1-n)}, \quad (5)$$

where Φ is the sample porosity (-) derived from bulk density measurements as described in Section 2.4.3.

2.4.3. Organic matter and water retention measurements

After the incubation measurements, the samples were dried at 105 °C for 24 hours to obtain the final water content of each sample. A subsample was then ground in order to measure total organic matter content by loss-on-ignition. For this step, we followed the procedure outlined by Hogsteen et al. (2015), in which samples were heated at 550°C for 3 hours in a Nabertherm oven.

Independent samples were collected to determine water retention curves using a Richards's pressure plate apparatus. Samples were subjected to pressure heads ranging from 0 to 15,000 hPa, and corresponding changes in mass were recorded to calculate water content at each pressure step. Water retention data were fitted using the van Genuchten model (Van Genuchten, 1980) implemented in the soilphysics package (v. 5.0) in R (R Core Team, 2023). Model parameters (α and n) were estimated separately for each soil and structural treatment. The fitted retention functions were subsequently used to convert the applied pressure heads during the incubation experiment into corresponding volumetric water contents for each sample. The fitted water retention curves for all soil and structural treatments are provided in Fig. S4 of the Supplementary Material.

2.4.4. Statistical analysis and data visualisation

The statistical analysis and data visualization were conducted using RStudio (v. 4.3.0; R Core Team, 2023).

Overall variance across sampling sites and depths was tested using Type III ANOVA with Welch's correction and Satterthwaite's method for degrees of freedom, implemented via the ggstatsplot package to account for unbalanced data.

Finally, soil respiration rate was plotted as a function of sample tortuosity. Regression analyses were performed using linear mixed-effects models fitted with the nlme package to assess differences among sampling depths and field treatments.

3. Results

3.1. Soil respiration rates across soil matric potential and organic matter quantification

Organic matter (OM) content varied among individual soil samples (Fig. S3), ranging from approximately 3.6% to 14.1% of dry soil mass. The lowest OM content was observed in the sieved CT topsoil, whereas the highest values occurred in the undisturbed CT subsoil samples. However, OM content did not differ significantly among groups ($F_{statistic(7,\ 10.4)}$ = 1.96, p =

0.16). At the highest saturation level, a significant difference in total respiration rate was observed between sieved and undisturbed samples ($p < 0.03$), as well as between topsoil and subsoil samples ($p < 0.002$) (Table S2).

The relative respiration rate, normalized to the values measured at -70 hPa, increased by approximately three orders of magnitude as pressure head increased (i.e., became less negative) from -996 to -70 hPa (Fig. 1). For the sieved samples, this trend was maintained across all pressure heads, with a small respiration peak observed at -100 hPa. In contrast, the undisturbed samples exhibited a respiration peak at -250 hPa. This increase was particularly pronounced for the topsoil conservation agriculture (CA) sample.

Apart from this peak in the undisturbed samples, no significant differences were observed between sampling depths (topsoil versus subsoil) or field treatments (CT versus CA). Linear mixed-effects modelling indicated a significant effect of pressure head on respiration flux ($p = 0.0008$), but no significant effects of sample structure ($p = 0.178$), field treatment ($p = 0.436$), or their interactions.

In addition, no significant difference in relative respiration flux was detected between -996 and -630 hPa ($p > 0.618$). Post hoc comparisons further confirmed that relative respiration flux did not differ significantly among pressure heads beyond -450 hPa ($p = 0.311$).

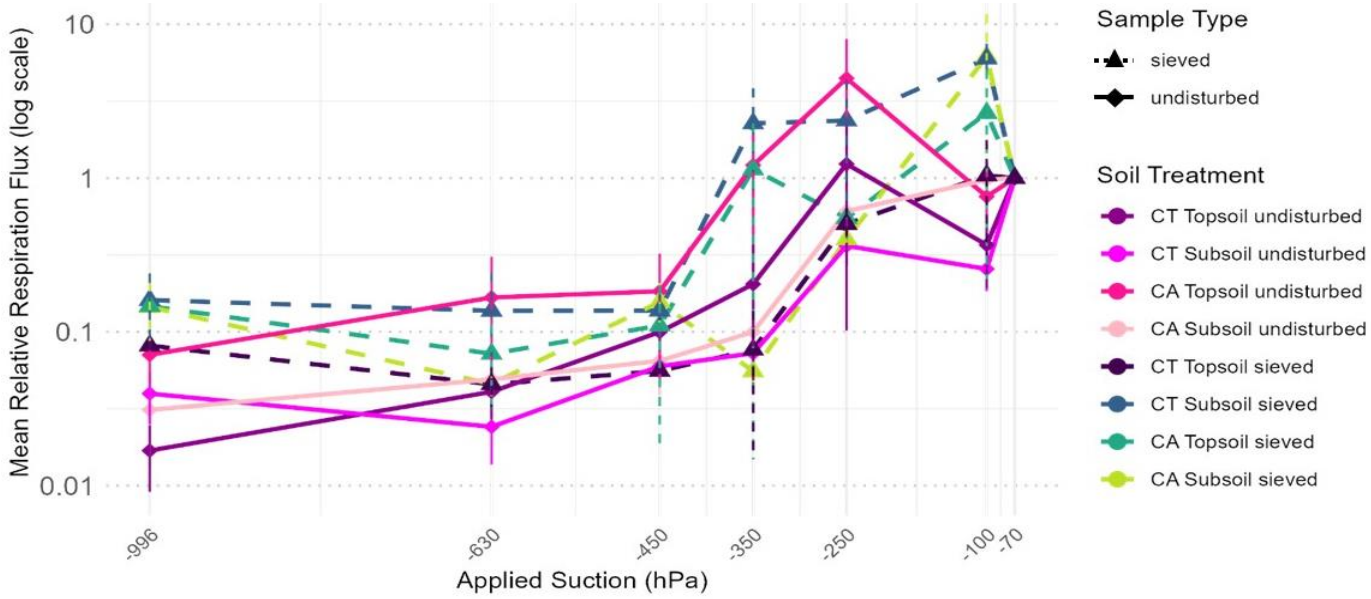

Figure 1: Mean relative soil respiration flux obtained from the triplicate of each treatment measured at a range of different Applied Suctions (hPa). The different suction levels represent soil matric potentials analysed throughout the study. The sample abbreviation CA stands for conservation agriculture field treatment and CT stands for conventional tillage. The solid lines represent undisturbed soil cores while the dashed line corresponds to sieved samples. The relative respiration rate is normalised to the respiration rate observed at -70 hPa, corresponding to our highest tested saturation, and is represented in a log scale. The error bars exceeding the marker size point are shown. For more details on averages and standard deviation of the mean, please consult Table S3 of our supplementary materials.

3.2. Soil electrical conductivity across soil water content

Electrical conductivity (EC) measurements did not differ significantly between electrode channels within samples. Higher values were observed in the sieved conventional tillage (CT) topsoil (1052 μS cm^{-1}) and subsoil (742 μS cm^{-1}). Results for the conventional tillage (CT) samples are shown in Fig. 2, while the corresponding results for CA soils are provided in Fig. S5 of the Supplementary Material.

Across both CT and conservation agriculture (CA) systems, EC increased systematically with increasing water saturation (Fig. 2; Fig. S5). Although variability among individual cores was observed, no consistent separation between undisturbed and sieved treatments was evident across the full saturation range. Likewise, differences between topsoil and subsoil samples were not systematic. Two-way ANOVA applied to the fitted Archie saturation exponent (*n*, log-transformed) confirmed the absence of significant effects of depth, soil structure, or their interaction in either system (CT: depth $p = 0.72$, structure $p = 0.26$, interaction $p = 0.68$; CA: depth $p = 0.89$, structure $p = 0.77$, interaction $p = 0.90$).

In the undisturbed CT treatment, one replicate in both topsoil and subsoil showed a steeper decline in EC with decreasing water saturation (Fig. 2), leading to greater variability in the fitted EC-S_w relationships. This pattern was not observed in the CA samples or in other depth-structure combinations.

The EC-derived tortuosity factor (τ_w) increased with decreasing water saturation for all samples (Fig. 2; Fig. S5), reflecting progressively reduced diffusive transport at lower saturation levels. Although undisturbed samples exhibited greater variability across the saturation range, two-way ANOVA applied to log-transformed τ_w revealed no significant effects of depth, soil structure, or their interaction in either management system (CT: depth $p = 0.57$, structure $p = 0.22$, interaction $p = 0.55$; CA: depth $p = 0.62$, structure $p = 0.56$, interaction $p = 0.64$). Similar results were obtained when τ_w values derived from the fitted curves were compared at $S_w = 0.3$, 0.5, and 0.8 for both management systems.

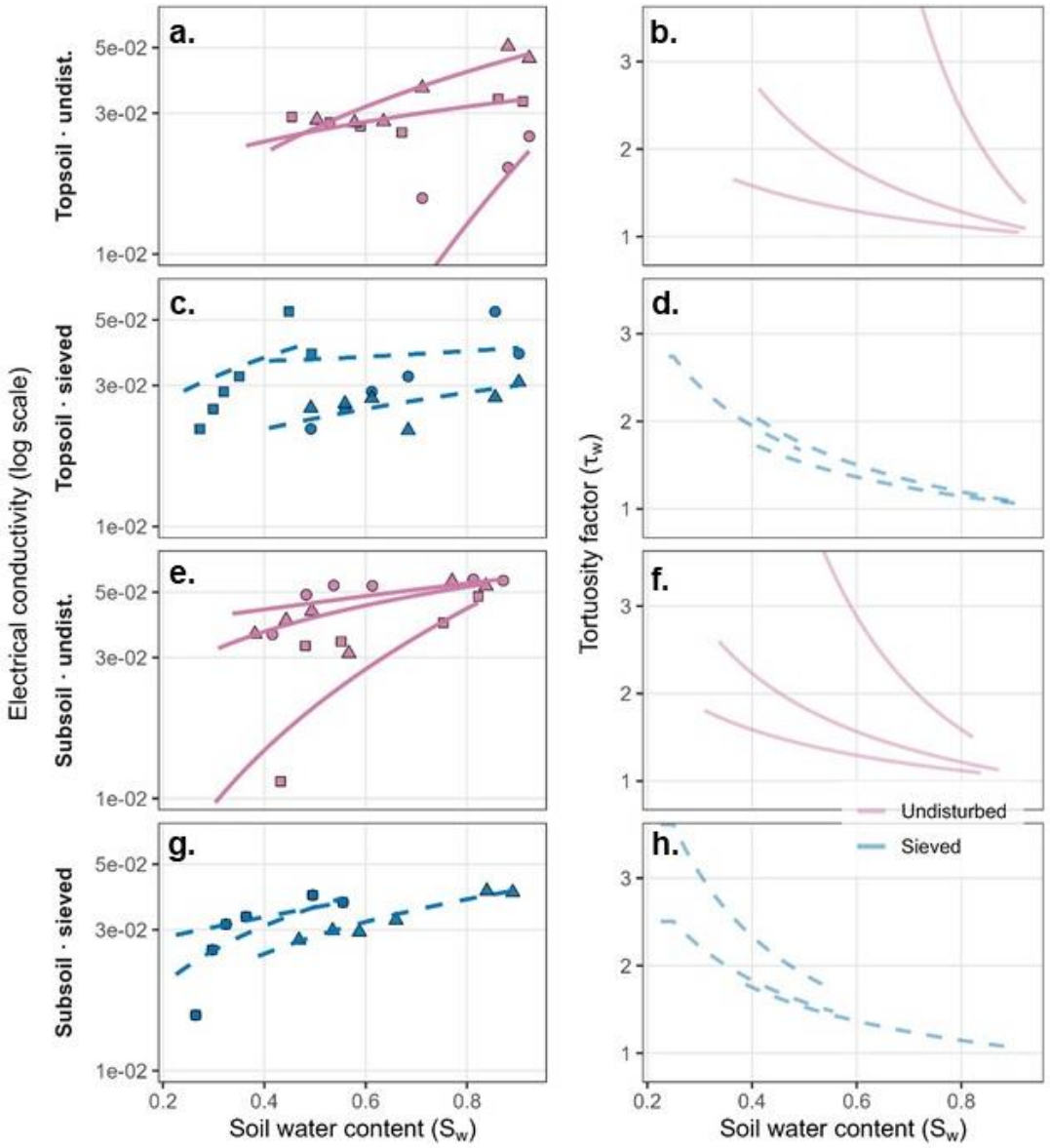

Figure 2: Electrical conductivity and derived tortuosity as a function of water saturation for soils under conventional tillage (CT) and conservation agriculture (CA). (a, c, e, g) Bulk electrical conductivity (EC) plotted against water saturation (S_w) for topsoil and subsoil samples under undisturbed and sieved conditions. EC is shown on a logarithmic scale. Points represent measured values for individual soil cores, while lines represent fits of the pedophysical model (Eq. 4) applied separately to each core. Variability among individual cores resulted in differences in model fit quality for some samples. (b, d, f, h) Corresponding tortuosity factor (τ_w) derived from EC measurements using Eq. 5. Solid lines indicate undisturbed soils and dashed lines indicate sieved soils. Model parameter estimates are provided in Table S5. The full dataset and corresponding fitted curves for all samples are provided in the Supplementary Material.

3.3. Relationship between respiration flux and tortuosity factor

To evaluate whether respiration flux was coupled to diffusive transport constraints, linear regressions were fitted on $\log_{10}$-transformed respiration flux and $\log_{10}$-transformed EC-derived tortuosity (τ_w) for both CT and CA samples (Fig. 3, Fig. S6 for CA).

In the CT samples, respiration flux was negatively related to τ_w. Linear regressions were fitted using individual measurements from each soil core across the range of water saturations. A linear model including depth and structure confirmed a significant interaction between τ_w and soil structure ($p<0.001$), indicating that slopes differed between undisturbed and sieved samples. No significant interaction with depth was observed. Slopes and coefficients of determination for each depth-structure combination are summarised in Table S6.

In the CA samples, a significant overall negative relationship between respiration flux and τ_w was also observed ($F_{statistic(1, 58)} = 5.08$, $p = 0.028$). However, neither depth ($p = 0.90$) nor soil structure ($p = 0.72$), nor their interactions with τ_w significantly influenced the slope of the relationship. These results indicate that respiration decreased with increasing tortuosity in both management systems, although structural effects were only detectable in the CT samples.

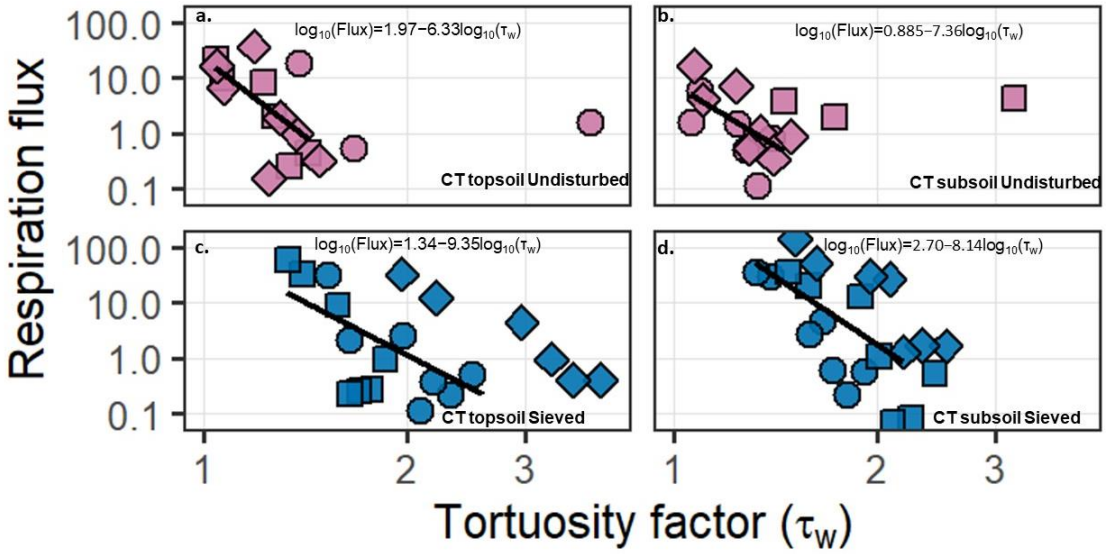

Fig. 3: Relationship between soil respiration flux and EC-derived tortuosity (τ_w) for the conventional tillage (CT) samples. Panels (a-b) show undisturbed samples and panels (c-d) show sieved samples. The left column corresponds to topsoil and the right column to subsoil. Points represent individual measurements from soil cores, with symbol shape indicating replicate. Respiration flux is plotted on a logarithmic scale. Solid black lines represent linear regressions fitted between log10-transformed respiration flux and log10-transformed tortuosity (τ_w) within the diffusion-limited range used for the statistical analysis. Only measurements within this range were included in the regressions. Regression equations are shown in each panel.

4. Discussion

4.1. Electrical conductivity as a proxy of soil respiration

We hypothesised that decreasing matric potential would be associated with reductions in both CO_2 flux and EC, reflecting reduced aqueous phase connectivity within the pore network (Fig. 3). Reduced water availability is known to increase hydraulic and electrical tortuosity, thereby constraining diffusive transport (Ghanbarian et al., 2013; Revil & Jougnot, 2008). Consistent with this conceptual framework, both EC and soil respiration decreased as the soils dried. These declines were accompanied by an increase in τ_w with decreasing water saturation (Fig. 2).

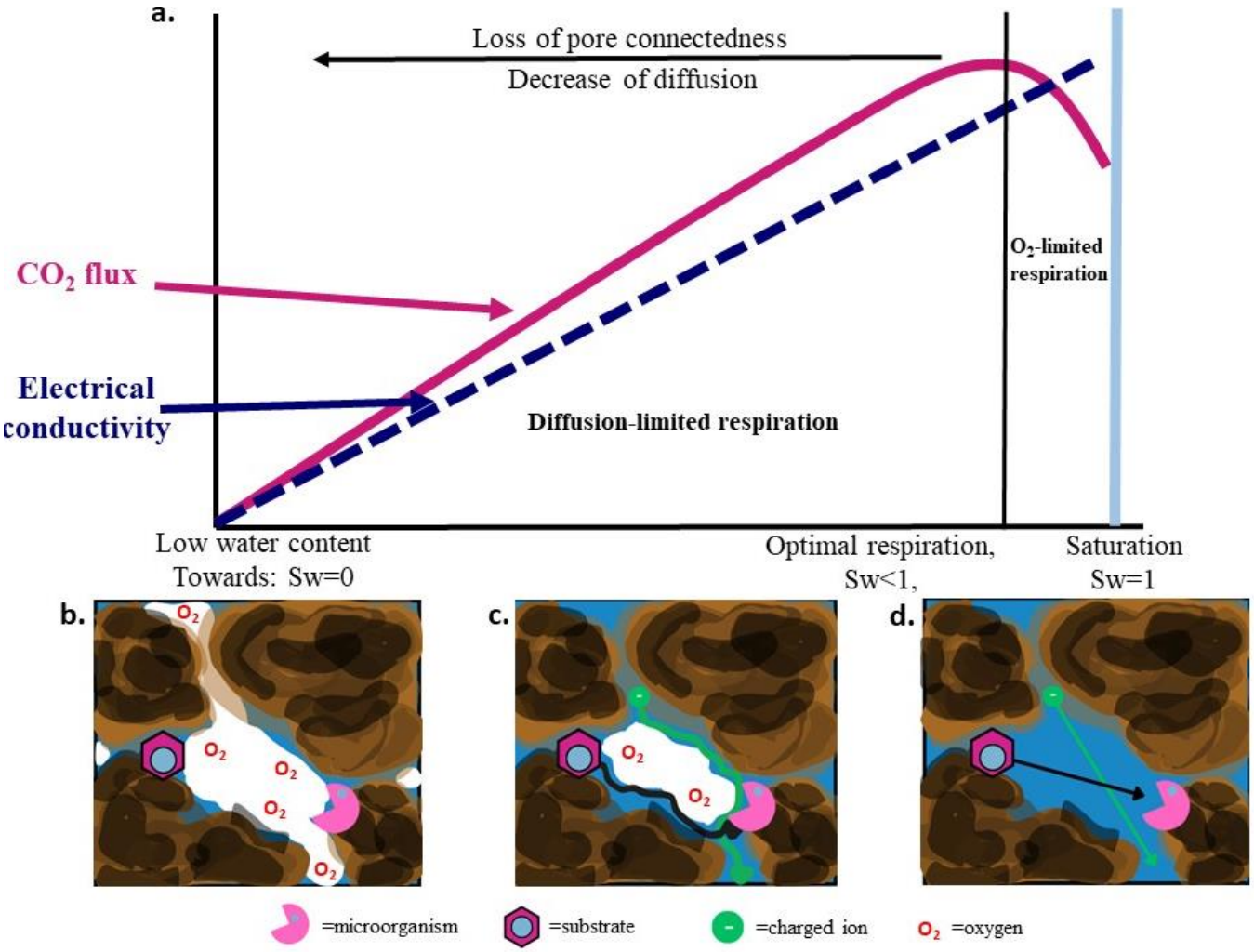

Figure 4: Conceptual framework linking soil respiration and electrical conductivity to water saturation. (a) Schematic representation of soil respiration (CO_2 flux) and bulk electrical conductivity (EC) as a function of water saturation (S_w). As

saturation decreases from near saturation (S_w = 1) toward lower water contents, EC declines approximately monotonically due to reduced pore-water connectivity. In contrast, respiration shows a non-linear response: at high saturation, respiration is limited by oxygen diffusion; at intermediate saturation, respiration is maximized where oxygen supply and substrate connectivity are balanced; and at low saturation, respiration becomes diffusion-limited due to reduced aqueous connectivity and restricted solute transport. (b-d) Conceptual pore-scale illustrations corresponding to low water content (b), intermediate (optimal) saturation (c), and near-saturated conditions (d). The schematics show changes in microorganism–substrate–oxygen interactions and conductive pathways along the saturation gradient. Symbols represent microorganisms, substrates, charged ions, and oxygen as indicated.

Respiration peaked at -250 hPa in the undisturbed samples and did not increase further at higher saturation levels. Because respiration near saturation may reflect oxygen limitation rather than substrate diffusion, the highest saturation levels were excluded from the regression analyses linking respiration and tortuosity (Fig. 3). This plateau likely reflects reduced oxygen diffusion under near-saturated conditions, as oxygen diffuses more slowly through water than through air (Moyano et al., 2013). Only measurements within the diffusion-limited range below this peak were therefore included in the regression analyses, and this exclusion was applied consistently across structural treatments to ensure comparability.

An increase in respiration flux was observed at -250 hPa in the undisturbed samples. At higher saturation levels (−250 to 0 hPa in undisturbed samples and -100 to 0 hPa in sieved samples), respiration did not increase further. This plateau may reflect reduced oxygen diffusion under near-saturated conditions, as oxygen diffuses more slowly through water than through air (Moyano et al., 2013). Similar non-monotonic responses of respiration to water content have been reported across soil types (Ebrahimi & Or, 2015; Moyano et al., 2013), suggesting the presence of a moisture range where oxygen supply and substrate diffusion are balanced.

Below this moisture range, respiration declined with decreasing water content. At lower saturation, reduced water availability increases tortuosity and constrained diffusive transport (Ebrahimi & Or, 2015; Ghezzehei et al., 2019). In this regime, EC and the derived tortuosity factor (τ_w) reflect changes in the geometry of the conductive phase and therefore provide information on conditions affecting diffusive transport (Revil & Jougnot, 2008; Jougnot et al., 2009).

A general decrease in EC with decreasing water saturation was observed in most samples (Fig. 2). This pattern is consistent with reduced connectivity of the water phase within the pore system, which increases electrical tortuosity and lengthens transport pathways (Ghanbarian et al., 2013; Jougnot et al., 2018). At sufficiently low saturation, the water phase approaches a percolation threshold where conductive pathways become increasingly disconnected (Hunt, 2005; Revil & Jougnot, 2008). Because solute and substrate diffusion occur primarily through the aqueous phase, this progressive loss of connectivity supports the interpretation that decreasing water saturation constrains microbial respiration through diffusion limitation.

Interestingly, at the second lowest water content in the conventional tillage subsoil samples, EC showed an unexpected increase. A clear physical explanation is not evident; however, fungal growth was observed on the sample surface during the incubation period. Although speculative, fungal activity may have contributed to this isolated increase in EC. Fungal hyphae can modify their surrounding microenvironment through both chemical and physical processes, including mobilisation of

phosphate ions and aggregate formation(Ameen et al., 2019; Hartmann & Six, 2022; Sun et al., 2022). Such local changes in pore-water chemistry or structure could influence measured conductivity. This feature was not observed in other depths or management systems, and therefore remains tentative.

In several cases, respiration did not differ significantly between the two lowest water saturations (Fig. 1). This is consistent with reports of sigmoidal declines in respiration with decreasing water availability, where reductions may be gradual across specific matric potential ranges (Curiel Yuste et al., 2007; Ghezzehei et al., 2019).

4.2. Impact of soil structure on the respiration-tortuosity relationship

The significant log-log relationship between respiration flux and EC-derived tortuosity (τ_w) observed within the diffusion-limited range (Fig. 3) indicates a coupling between microbial respiration and diffusive transport constraints. In the CT samples, steeper slopes were observed for sieved soils relative to undisturbed soils, suggesting that under homogenised structural conditions respiration responded more strongly to changes in tortuosity. This contrast was not evident in the CA samples.

We hypothesized that sieving would alter pore structure by producing a more homogeneous pore network, leading to a more uniform decline in EC and respiration compared to undisturbed samples. However, while sieving significantly affected respiration rates, this was not reflected in bulk EC values. Instead, the EC-derived tortuosity (τ_w) showed a more homogeneous response to water saturation in the sieved samples (Fig. 2d and h), consistent with a more uniform pore network following soil homogenisation. Respiration rates were also higher in sieved samples near saturation (Fig. 1). Our findings align with Herbst et al. (2016) who reported similar contrasts between sieved and undisturbed cores across a range of water contents.

Two mechanisms may explain the differences between sieved and undisturbed samples. First, sieving alters pore size distribution, modifying hydraulic connectivity and drainage behaviour (Castellini & Ventrella, 2012; Shaxson, 2006). Smaller and more uniformly distributed pores may retain water longer during drying, reinforcing contrasts between structural treatments at intermediate matric potentials (Çelik et al., 2021; Gupta Choudhury et al., 2014).

Second, sieving can affect carbon availability to microbial decomposers. The physical protection of organic C from microbial decomposition is believed to be a major mechanism leading to organic C persisting in soil (Moyano et al., 2013; Six et al., 2006). Sieving may disrupt this protection by breaking aggregates and increasing contact between substrates and microbial communities. Improved aeration and substrate availability in sieved samples may therefore explain why soil respiration remains elevated even close to complete saturation. The subsequent decline in respiration beyond the optimal matric potential further supports moisture limitation of decomposition (Crawford, 2005; Fan et al., 2015). The absence of significant differences in EC between structural treatments indicates that sieving did not substantially alter bulk conductive properties. This difference in slopes indicates that soil structure influenced the sensitivity of respiration to tortuosity, even though τw itself did not differ significantly between structural treatments. Such decoupling between bulk physical transport metrics and biological response has previously been reported when bulk density and water content are comparable (Nadler, 1991).

4.3. Impact of agricultural treatment

Although there were no significant differences in either relative respiration rate or relative electrical conductivity between the management systems, differences emerged in how respiration responded to changes in water availability and tortuosity. In particular, undisturbed topsoil samples from the CT system maintained comparatively higher respiration rates at higher matric potentials relative to the corresponding CA samples. Conventional tillage disrupts soil aggregates and redistributes organic matter within the plough layer, potentially enhancing substrate accessibility and microbial activity in topsoil horizons (Franco-Luesma et al., 2020; Zsolt et al., 2020).The stronger structural effects observed in the CT samples, particularly in the respiration–τw relationship, are consistent with this mechanism, as respiration in sieved CT soils responded more strongly to changes in tortuosity than in undisturbed soils (Fig. 3). In contrast, the absence of comparable structural modulation in the CA samples suggests that long-term aggregate stability may buffer respiration responses to changes in tortuosity.

4.4. Effects of topsoil compared to subsoil

We hypothesized that respiration-EC relationships would be weaker in the topsoil than in the subsoil due to a more homogeneous distribution of organic matter and therefore reduced diffusion dependence. However, no significant differences were detected. Because organic matter contents were similar between depths, substrate availability was likely comparable, and depth-related differences in diffusion dependence could not be resolved.

Nevertheless, respiration rates in the topsoil were higher than in the subsoil at high moisture levels, indicating greater mineralisation potential under near-optimal conditions. As the soils dried, the respiration rates in the topsoil and subsoil converged, suggesting that diffusion limitation increasingly constrained activity and masked depth-related differences. In sieved samples, this convergence between depths was less apparent, possibly because homogenisation reduced structural and substrate heterogeneity, thereby altering microbial access to organic matter (Salomé et al., 2010).

5. Conclusion

This study evaluated whether electrical conductivity (EC) measurements can serve as a proxy for soil respiration under diffusion-limited conditions, given the shared dependence of both processes on water-phase connectivity. Across soils differing in structure, depth, and management history, respiration decreased with declining water availability and increasing tortuosity. Log-log regressions revealed significant relationships between respiration flux and EC-derived tortuosity (τ_w), indicating that EC reflects transport constraints governing microbial activity. These findings suggest that EC provides quantitative information on diffusion-limited respiration in the absence of substantial advective water flow.

Structural treatments influenced the strength of the respiration-τ_w relationship, particularly in conventionally tilled soils, highlighting the role of pore-network organisation and substrate accessibility in modulating diffusion constrain**ts**.

Overall, the results support the interpretation that soil respiration is partly diffusion-limited under unsaturated conditions and that this limitation can be captured using EC-derived transport metrics. Future work should evaluate the robustness of this

approach under field conditions and refine the quantitative framework linking EC-derived transport metrics to microbial process rates.

Author contribution

The experimental conceptualization was a collaboration between all co-authors. Funding acquisition, project management and supervision: DJ and NN; initial methodology development and validation: MG, OF; Investigation, Formal analysis: OF; Visualization: OF, DJ, NN; Writing: First draft: OF; Rewriting and editing: NN, DJ, OF

Code and data availability

The datasets supporting this study, including respiration and electrical conductivity measurements, are available as assets associated with this manuscript submission. Supplementary material containing additional methodological details is provided with the manuscript. Custom R scripts used for data processing, statistical analyses, and figure generation are available from the corresponding author upon reasonable request.

Competing interests

The authors declare that they have no conflict of interest.

Acknowledgements

The authors want to thank F. Delarue for his help with loss-on-ignition measurement. The authors also thank the reviewers and editor for their constructive comments, which helped improve the manuscript.

Financial support

The PhD thesis O. Fülöp is supported by the BIOMASS project funded by the 80|PRIME program of the CNRS MITI.

References:

Allende-Montalbán, R., San-Juan-Heras, R., Martín-Lammerding, D., Delgado, M. D. M., Albarrán, M. D. M., & Gabriel, J. L. (2024). The soil sample conservation method and its potential impact on ammonium, nitrate and total mineral nitrogen measurements. *Geoderma*, *448*, 116963. https://doi.org/10.1016/j.geoderma.2024.116963

Al-Maliki, S., & Ebreesum, H. (2020). Changes in soil carbon mineralization, soil microbes, roots density and soil structure following the application of the arbuscular mycorrhizal fungi and green algae in the arid saline soil. *Rhizosphere*, *14*, 100203. https://doi.org/10.1016/j.rhisph.2020.100203

Ameen, F., AlYahya, S. A., AlNadhari, S., Alasmari, H., Alhoshani, F., & Wainwright, M. (2019). Phosphate solubilizing bacteria and fungi in desert soils: Species, limitations and mechanisms. *Archives of Agronomy and Soil Science*, *65*(10), 1446–1459. https://doi.org/10.1080/03650340.2019.1566713

Autret, B., Guillier, H., Pouteau, V., Mary, B., & Chenu, C. (2020). Similar specific mineralization rates of organic carbon and nitrogen in incubated soils under contrasted arable cropping systems. *Soil and Tillage Research*, *204*, 104712. https://doi.org/10.1016/j.still.2020.104712

Autret, B., Mary, B., Chenu, C., Balabane, M., Girardin, C., Bertrand, M., Grandeau, G., & Beaudoin, N. (2016). Alternative arable cropping systems: A key to increase soil organic carbon storage? Results from a 16 year field experiment. *Agriculture, Ecosystems & Environment*, *232*, 150–164. https://doi.org/10.1016/j.agee.2016.07.008

Bellone, D., Jeuffroy, M.-H., Bertrand, M., Mistou, M.-N., Barbu, C., Ballini, E., Morison-Valantin, M., Gauffreteau, A., & Pashalidou, F. G. (2023). Are innovative cropping systems less dependent on synthetic pesticides to treat Septoria leaf blotch (Zymoseptoria tritici) than conventional systems? *Crop Protection*, *170*, 106266. https://doi.org/10.1016/j.cropro.2023.106266

Blanchy, G., Deroo, W., De Swaef, T., Lootens, P., Quataert, P., Roldán-Ruíz, I., Versteeg, R., & Garré, S. (2025). Closing the phenotyping gap with non-invasive belowground field phenotyping. *SOIL*, *11*(1), 67–84. https://doi.org/10.5194/soil-11-67-2025

Castellini, M., & Ventrella, D. (2012). Impact of conventional and minimum tillage on soil hydraulic conductivity in typical cropping system in Southern Italy. *Soil and Tillage Research*, *124*, 47–56. https://doi.org/10.1016/j.still.2012.04.008

Çelik, İ., Günal, H., Acir, N., Barut, Z. B., & Budak, M. (2021). Soil quality assessment to compare tillage systems in Cukurova Plain, Turkey. *Soil and Tillage Research*, *208*, 104892. https://doi.org/10.1016/j.still.2020.104892

Chabert, A., & Sarthou, J.-P. (2020). Conservation agriculture as a promising trade-off between conventional and organic agriculture in bundling ecosystem services. *Agriculture, Ecosystems & Environment*, *292*, 106815. https://doi.org/10.1016/j.agee.2019.106815

Colas, E. (n.d.). *Impact de l'humidité et des solutions salines sur le comportement dimensionnel de grès du Buntsandstein :*

Cosentino, D., Chenu, C., & Le Bissonnais, Y. (2006). Aggregate stability and microbial community dynamics under drying–wetting cycles in a silt loam soil. *Soil Biology and Biochemistry*, *38*(8), 2053–2062. https://doi.org/10.1016/j.soilbio.2005.12.022

Crawford, R. L. (2005). Microbial Diversity and Its Relationship to Planetary Protection. *Applied and Environmental Microbiology*, *71*(8), 4163–4168. https://doi.org/10.1128/AEM.71.8.4163-4168.2005

Crowther, T. W., Van Den Hoogen, J., Wan, J., Mayes, M. A., Keiser, A. D., Mo, L., Averill, C., & Maynard, D. S. (2019). The global soil community and its influence on biogeochemistry. *Science*, *365*(6455), eaav0550. https://doi.org/10.1126/science.aav0550

Curiel Yuste, J., Baldocchi, D. D., Gershenson, A., Goldstein, A., Misson, L., & Wong, S. (2007). Microbial soil respiration and its dependency on carbon inputs, soil temperature and moisture. *Global Change Biology*, *13*(9), 2018–2035. https://doi.org/10.1111/j.1365-2486.2007.01415.x

Davidson, EriC. A., Belk, E., & Boone, R. D. (1998). Soil water content and temperature as independent or confounded factors controlling soil respiration in a temperate mixed hardwood forest. *Global Change Biology*, *4*(2), 217–227. https://doi.org/10.1046/j.1365-2486.1998.00128.x

Dignac, M.-F., Derrien, D., Barré, P., Barot, S., Cécillon, L., Chenu, C., Chevallier, T., Freschet, G. T., Garnier, P., Guenet, B., Hedde, M., Klumpp, K., Lashermes, G., Maron, P.-A., Nunan, N., Roumet, C., & Basile-Doelsch, I. (2017). Increasing soil carbon storage: Mechanisms, effects of agricultural practices and proxies. A review. *Agronomy for Sustainable Development*, *37*(2), 14. https://doi.org/10.1007/s13593-017-0421-2

Dubey, R. K., Tripathi, V., Prabha, R., Chaurasia, R., Singh, D. P., Rao, Ch. S., El-Keblawy, A., & Abhilash, P. C. (2020). *Unravelling the Soil Microbiome: Perspectives For Environmental Sustainability*. Springer International Publishing. https://doi.org/10.1007/978-3-030-15516-2

Ebrahimi, A., & Or, D. (2015). Hydration and diffusion processes shape microbial community organization and function in model soil aggregates. *Water Resources Research*, *51*(12), 9804–9827. https://doi.org/10.1002/2015WR017565

Fan, L.-C., Yang, M.-Z., & Han, W.-Y. (2015). Soil Respiration under Different Land Uses in Eastern China. *PLOS ONE*, *10*(4), e0124198. https://doi.org/10.1371/journal.pone.0124198

Franco-Luesma, S., Cavero, J., Plaza-Bonilla, D., Cantero-Martínez, C., Arrúe, J. L., & Álvaro-Fuentes, J. (2020). Tillage and irrigation system effects on soil carbon dioxide (CO2) and methane (CH4) emissions in a maize monoculture under Mediterranean conditions. *Soil and Tillage Research*, *196*, 104488. https://doi.org/10.1016/j.still.2019.104488

Garre, S., Deswaef, T., Borra-Serrano, I., Lootens, P., & Blanchy, G. (2021). The potential of electrical imaging for field root zone phenotyping. *NSG2021 27th European Meeting of Environmental and Engineering Geophysics*, 1–5. https://doi.org/10.3997/2214-4609.202120221

Ghanbarian, B., Hunt, A. G., Ewing, R. P., & Sahimi, M. (2013). Tortuosity in Porous Media: A Critical Review. *Soil Science Society of America Journal*, *77*(5), 1461–1477. https://doi.org/10.2136/sssaj2012.0435

Ghezzehei, T. A., Sulman, B., Arnold, C. L., Bogie, N. A., & Berhe, A. A. (2019). On the role of soil water retention characteristic on aerobic microbial respiration. *Biogeosciences*, *16*(6), 1187–1209. https://doi.org/10.5194/bg-16-1187-2019

Greenspan, L. (1977). Humidity fixed points of binary saturated aqueous solutions. *Journal of Research of the National Bureau of Standards Section A: Physics and Chemistry*, *81A*(1), Article 1. https://doi.org/10.6028/jres.081A.011

Gupta Choudhury, S., Srivastava, S., Singh, R., Chaudhari, S. K., Sharma, D. K., Singh, S. K., & Sarkar, D. (2014). Tillage and residue management effects on soil aggregation, organic carbon dynamics and yield attribute in rice–wheat cropping system under reclaimed sodic soil. *Soil and Tillage Research*, *136*, 76–83. https://doi.org/10.1016/j.still.2013.10.001

Hargreaves, S. K., Williams, R. J., & Hofmockel, K. S. (2015). Environmental Filtering of Microbial Communities in Agricultural Soil Shifts with Crop Growth. *PLOS ONE*, *10*(7), e0134345. https://doi.org/10.1371/journal.pone.0134345

Hartmann, M., & Six, J. (2022). Soil structure and microbiome functions in agroecosystems. *Nature Reviews Earth & Environment*, *4*(1), 4–18. https://doi.org/10.1038/s43017-022-00366-w

Henneron, L., Bernard, L., Hedde, M., Pelosi, C., Villenave, C., Chenu, C., Bertrand, M., Girardin, C., & Blanchart, E. (2015). Fourteen years of evidence for positive effects of conservation agriculture and

organic farming on soil life. *Agronomy for Sustainable Development*, *35*(1), 169–181. https://doi.org/10.1007/s13593-014-0215-8

Herbst, M., Tappe, W., Kummer, S., & Vereecken, H. (2016). The impact of sieving on heterotrophic respiration response to water content in loamy and sandy topsoils. *Geoderma*, *272*, 73–82. https://doi.org/10.1016/j.geoderma.2016.03.002

Hermans, T., Goderniaux, P., Jougnot, D., Fleckenstein, J. H., Brunner, P., Nguyen, F., Linde, N., Huisman, J. A., Bour, O., Lopez Alvis, J., Hoffmann, R., Palacios, A., Cooke, A.-K., Pardo-Álvarez, Á., Blazevic, L., Pouladi, B., Haruzi, P., Fernandez Visentini, A., Nogueira, G. E. H., … Le Borgne, T. (2023). Advancing measurements and representations of subsurface heterogeneity and dynamic processes: Towards 4D hydrogeology. *Hydrology and Earth System Sciences*, *27*(1), 255–287. https://doi.org/10.5194/hess-27-255-2023

Hunt, A. G. (2005). Continuum percolation theory for transport properties in porous media. *Philosophical Magazine*, *85*(29), 3409–3434. https://doi.org/10.1080/14786430500157094

Jougnot, D., Jiménez-Martínez, J., Legendre, R., Le Borgne, T., Méheust, Y., & Linde, N. (2018). Impact of small-scale saline tracer heterogeneity on electrical resistivity monitoring in fully and partially saturated porous media: Insights from geoelectrical milli-fluidic experiments. *Advances in Water Resources*, *113*, 295–309. https://doi.org/10.1016/j.advwatres.2018.01.014

Jougnot, D., Revil, A., & Leroy, P. (2009). Diffusion of ionic tracers in the Callovo-Oxfordian clay-rock using the Donnan equilibrium model and the formation factor. *Geochimica et Cosmochimica Acta*, *73*(10), 2712–2726. https://doi.org/10.1016/j.gca.2009.01.035

Juarez, S., Nunan, N., Duday, A.-C., Pouteau, V., & Chenu, C. (2013). Soil carbon mineralisation responses to alterations of microbial diversity and soil structure. *Biology and Fertility of Soils*, *49*(7), 939–948. https://doi.org/10.1007/s00374-013-0784-8

Kpemoua, T. P. I., Leclerc, S., Barré, P., Houot, S., Pouteau, V., Plessis, C., & Chenu, C. (2023). Are carbon-storing soils more sensitive to climate change? A laboratory evaluation for agricultural temperate soils. *Soil Biology and Biochemistry*, *183*, 109043. https://doi.org/10.1016/j.soilbio.2023.109043

Loiseau, B., Carrière, S. D., Jougnot, D., Singha, K., Mary, B., Delpierre, N., Guérin, R., & Martin-StPaul, N. K. (2023). The geophysical toolbox applied to forest ecosystems – A review. *Science of The Total Environment*, *899*, 165503. https://doi.org/10.1016/j.scitotenv.2023.165503

Lützow, M. V., Kögel-Knabner, I., Ekschmitt, K., Matzner, E., Guggenberger, G., Marschner, B., & Flessa, H. (2006). Stabilization of organic matter in temperate soils: Mechanisms and their relevance under different soil conditions – a review. *European Journal of Soil Science*, *57*(4), 426–445. https://doi.org/10.1111/j.1365-2389.2006.00809.x

Mondal, S., & Chakraborty, D. (2022). Global meta-analysis suggests that no-tillage favourably changes soil structure and porosity. *Geoderma*, *405*, 115443. https://doi.org/10.1016/j.geoderma.2021.115443

Moyano, F. E., Manzoni, S., & Chenu, C. (2013). Responses of soil heterotrophic respiration to moisture availability: An exploration of processes and models. *Soil Biology and Biochemistry*, *59*, 72–85. https://doi.org/10.1016/j.soilbio.2013.01.002

Nadler, A. (1991). EFFECT OF SOIL STRUCTURE ON BULK SOIL ELECTRICAL CONDUCTIVITY (ECa) USING THE TDR AND 4P TECHNIQUES. *152(3)*, 199–203.

Nasiri, S., Andalibi, B., Tavakoli, A., Delavar, M. A., El-Keblawy, A., Zwieten, L. V., & Mastinu, A. (2023). The Mineral Biochar Alters the Biochemical and Microbial Properties of the Soil and the Grain Yield of Hordeum vulgare L. under Drought Stress. *Land*, *12*(3), 559. https://doi.org/10.3390/land12030559

Nunan, N., Schmidt, H., & Raynaud, X. (2020). *The ecology of heterogeneity: Soil bacterial communities and C dynamics.* Philosophical Transactions of the Royal Society B. https://doi.org/10.1098/rstb.2019.0249

Poll, C., Pagel, H., Devers-Lamrani, M., Martin-Laurent, F., Ingwersen, J., Streck, T., & Kandeler, E. (2010). Regulation of bacterial and fungal MCPA degradation at the soil–litter interface. *Soil Biology and Biochemistry*, *42*(10), 1879–1887. https://doi.org/10.1016/j.soilbio.2010.07.013

Ramoneda, J., Fan, K., Lucas, J. M., Chu, H., Bissett, A., Strickland, M. S., & Fierer, N. (2024). Ecological relevance of flagellar motility in soil bacterial communities. *The ISME Journal*, *18*(1), wrae067. https://doi.org/10.1093/ismejo/wrae067

Revil, A., & Jougnot, D. (2008). Diffusion of ions in unsaturated porous materials. *Journal of Colloid and Interface Science*, *319*(1), 226–235. https://doi.org/10.1016/j.jcis.2007.10.041

Salomé, C., Nunan, N., Pouteau, V., Lerch, T. Z., & Chenu, C. (2010). Carbon dynamics in topsoil and in subsoil may be controlled by different regulatory mechanisms: CARBON DYNAMICS IN TOPSOIL AND IN SUBSOIL. *Global Change Biology*, *16*(1), 416–426. https://doi.org/10.1111/j.1365-2486.2009.01884.x

Shaxson, T. F. (2006). Re-thinking the conservation of carbon, water and soil: A different perspective. *Agronomy for Sustainable Development*, *26*(1), 9–19. https://doi.org/10.1051/agro:2005054

Six, J., Frey, S. D., Thiet, R. K., & Batten, K. M. (2006). Bacterial and Fungal Contributions to Carbon Sequestration in Agroecosystems. *Soil Science Society of America Journal*, *70*(2), 555–569. https://doi.org/10.2136/sssaj2004.0347

Stanford, G., & Smith, S. J. (n.d.). *Nitrogen Mineralization Potentials of Soils*. Soil Science Society of America Journal. Retrieved https://doi.org/10.2136/sssaj1972.03615995003600030029x

Sun, R., Zhang, W., Liu, Y., Yun, W., Luo, B., Chai, R., Zhang, C., Xiang, X., & Su, X. (2022). Changes in phosphorus mobilization and community assembly of bacterial and fungal communities in rice rhizosphere under phosphate deficiency. *Frontiers in Microbiology*, *13*, 953340. https://doi.org/10.3389/fmicb.2022.953340

Van Genuchten, M. Th. (1980). A Closed-form Equation for Predicting the Hydraulic Conductivity of Unsaturated Soils. *Soil Science Society of America Journal*, *44*(5), 892–898. https://doi.org/10.2136/sssaj1980.03615995004400050002x

Waxman, M. H., & Smits, L. J. M. (1968). Electrical Conductivities in Oil-Bearing Shaly Sands. *Society of Petroleum Engineers Journal*, *8*(02), 107–122. https://doi.org/10.2118/1863-A

Zsolt, S., Tállai, M., Kincses, I., László, Z., Kátai, J., & Vágó, I. (2020). Effect of various soil cultivation methods on some microbial soil properties. *DRC Sustainable Future: Journal of Environment, Agriculture, and Energy*, *1*(1), 14–20. https://doi.org/10.37281/DRCSF/1.1.3